This item is likely protected under Title 17 of the U.S. Copyright Law. Unless on a Creative Commons license, for uses protected by Copyright Law, contact the copyright holder or the author.

Access to this work was provided by the University of Maryland, Baltimore County (UMBC) ScholarWorks@UMBC digital repository on the Maryland Shared Open Access (MD-SOAR) platform.

Please provide feedback

Please support the ScholarWorks@UMBC repository by emailing scholarworks-group@umbc.edu and telling us what having access to this work means to you and why it's important to you. Thank you.

Please do not adjust margins

Nanoscale

ARTICLE

Controlled Etching and Tapering of Au Nanorods using Cysteamine

Brian Szychowski,*[a] Haixu Leng, [b] Matthew Pelton,[b] and Marie-Christine Daniel[a]

Received 00th January 20xx,
Accepted 00th January 20xx

DOI: 10.1039/x0xx00000x

www.rsc.org/

While gold nanorods (AuNRs) have found many applications due to their unique optical properties, a few challenges persist in their synthesis. Namely, it is often difficult to reproducibly synthesize AuNRs with specific and monodisperse sizes, especially at shorter aspect ratios. Here, we report a method of post-synthesis precise tailoring of AuNRs by etching with cysteamine. Cysteamine selectively etches AuNRs from their ends while preserving the initial rod shape and monodispersity, making this a viable means of obtaining highly monodisperse short AuNRs down to aspect ratio 2.3. Further, we explore the effect of this etching method on two types of silica-coated AuNRs: silica side-coated and silica end-coated AuNRs. We find that the etching process is cysteamine concentration-dependent and can lead to different degrees of sharpening of the silica-coated AuNRs, forming elongated tips. We also find that cysteamine behaves only as a ligand at concentrations above 200 mM, as no etching of the AuNRs is observed in this condition. Simulations show that excitation of plasmon resonances in these sharpened AuNRs produces local electric fields twice as strong as those produced by conventional AuNRs. Thus, cysteamine etching of AuNRs is shown to be an effective means of tailoring both the size and shape of AuNRs along with their corresponding optical properties. At the same time, the resulting cysteamine coating on the etched AuNRs displays terminal amino groups that allow for further functionalization of the nanorods.

Introduction

Gold nanorods (AuNRs) have attracted attention due to their potential wide-ranging applications, including as bioimaging and therapeutic agents,[1, 2] sensors,[3] drug delivery systems,[4, 5] for surface enhanced Raman spectroscopy (SERS),[6] information processing,[7] light harvesting,[8] photocatalysis[9] and the development of metamaterials.[10] The properties of AuNRs are highly dependent on not only the size of the particles, but also on the specific shape of their ends.[11-14] Gold nanorods are most commonly synthesized through a seed-mediated growth method,[14-16] which has been extensively investigated to improve yield and accessible size ranges.[17] However, due to the reaction's sensitivity to impurities and small differences in starting materials, the method often leads to batch-to-batch and person-to-person variation in the exact size of the AuNRs formed.[18] Thus, it can be difficult to obtain AuNRs possessing precise sizes, and therefore, control of their optical properties.

This challenge has led to the study of the post-synthesis modification of AuNRs, in order to more precisely tailor the properties for the desired application. This can be done either through controlled etching of AuNRs[19-26] or through further growth of the rods through reduction of additional gold.[27-29] Etching usually starts preferentially at the ends of the rods, leading to the shortening of rods with time until they eventually resemble spherical nanoparticles.[19-22] Growth also generally occurs preferentially at the ends of the rods, which has been used to create AuNRs possessing unique tip-morphologies including dumbbell shapes,[11] dog-bone structures,[28] arrow-head tips,[29] and nanocuboids.[30, 31] Arrow-head tips are a unique case which can continually be grown until the rods eventually transform into octahedra.[27] The reverse, making flat-tipped rods from arrow-head or dog-bone structures, is also possible.[32]

In this study, we describe a novel method of etching AuNRs using cysteamine. Cysteamine etching has been previously reported for gold nanospheres[33] as well as small gold nanoclusters.[34, 35] However, its effect on gold nanorods has not been studied. In contrast to existing methods, we find that cysteamine offers several advantages: 1) its use does not require harsh conditions[36] (*e.g.*, high temperature,[28, 37] acidic conditions,[38-40] or the presence of iodine[19, 20] or metal ions[23-25, 38, 41, 42]) frequently needed in current methods of AuNR etching, and 2) the etching reaction preserves the AuNR shape and does not lead to spherical nanoparticles. Furthermore, we study the etching process using silica-coated AuNRs (side-coated, end-coated, and with a complete shell) and demonstrate that under certain conditions, cysteamine etching leads to a tapering of the nanorods ends. Simulations reveal these sharpened AuNRs to have a greater surface plasmon field enhancement at the tips than conventional nanorods of similar sizes, making them potentially useful in the fields of optics and plasmonics.

[a] *Department of Chemistry and Biochemistry, University of Maryland, Baltimore County, Baltimore, Maryland 21250, United States.*
[b] *Department of Physics, University of Maryland, Baltimore County, Baltimore, Maryland 21250, United States.*

Electronic Supplementary Information (ESI) available: Detailed experimental procedures, Influence of temperature, concentration, and pH on rate of etching, TEM images of AuNRs etched longer than 24 hours, solvent comparison tests, mercaptopropionic acid control test, STEM image of "uncapped" AuNR. (PDF)
See DOI: 10.1039/x0xx00000x

Please do not adjust margins

Please do not adjust margins

Results and discussion

In this study, we investigate the effect of cysteamine on AuNRs with several types of coating (CTAB, silica side-coating, silica end-coating, full silica coating) as summarized in Figure 1. We find that, although cysteamine is generally considered only as a water-soluble thiol ligand that can displace a citrate or CTAB coating, it can also display some significant and controllable gold etching properties under specific conditions. Depending on the coating, the AuNRs react differently in the presence of cysteamine, and the reaction temperature as well as cysteamine concentration can also influence the final results.

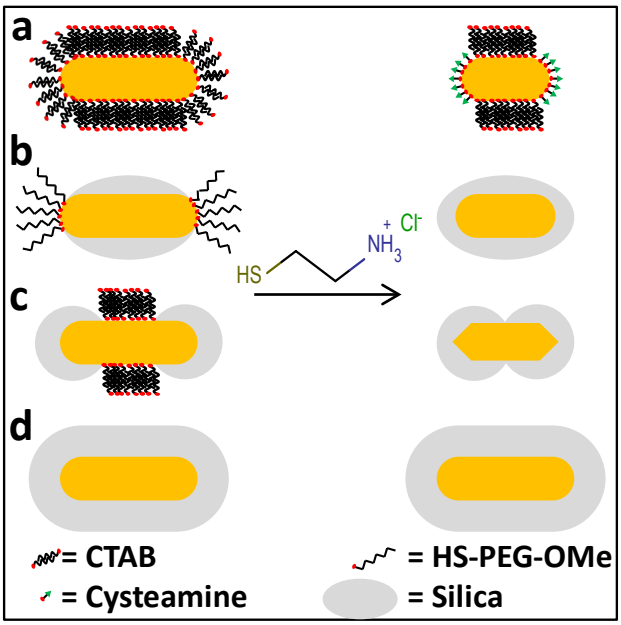

Figure 1. Scheme summarizing the different types of AuNRs used in this study and the resulting structures obtained after etching with 5 mM cysteamine. (a) CTAB-stabilized AuNRs, (b) silica side-coated AuNRs, (c) silica end-coated AuNRs, and (d) fully silica-coated AuNRs.

Cysteamine etching of CTAB-coated AuNRs

Figure 2 shows the results of cysteamine etching of CTAB-stabilized gold nanorods performed at 70°C using 5 mM cysteamine solution. In the absorption spectra, we observe no change in the transverse surface plasmon resonance (SPR) peak during the etching process; however, there is a steady blue shift in the longitudinal SPR peak with time, consistent with a shortening of the AuNRs. This was confirmed by transmission electron microscopy (TEM) imaging, where it was found that the average length of the rods decreased from 75 nm to 55 nm after 6 hours, whereas the width showed no significant change (26 nm to 23 nm). This corresponds to a decrease of the aspect ratio from 2.9 to 2.3. The preferential end-etching is consistent with previous reports investigating the etching of gold nanorods using different etchants.[19-22] It is believed that the difference in crystal structure as well as the lower packing density of CTAB at the ends of the rods make the ends more susceptible to etching, leading to a shortening of the rod and decrease in the longitudinal SPR peak wavelength.[29]

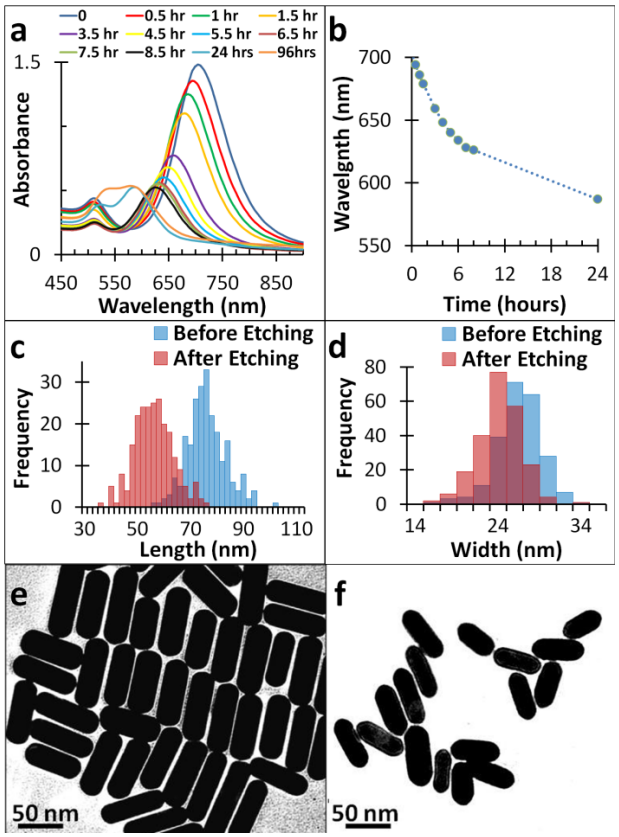

Figure 2. Etching of CTAB-stabilized AuNRs with 5 mM cysteamine at 70°C. **(a)** Evolution of AuNR absorption spectrum with time. **(b)** Change in longitudinal surface plasmon resonance peak position with time. **(c)** Distribution in AuNR length before and after etching. **(d)** Distribution in AuNR width before and after etching. **(e)** TEM image of AuNRs before etching. **(f)** TEM image of AuNRs after etching.

In contrast to existing etching techniques for gold nanorods, we do not observe either a linear decline of the longitudinal SPR peak with time until spherical particles are achieved, or the eventual complete dissolution of the gold.[19-22] Instead, we see an approximately linear decline for the first 8 hours, during which the wavelength of the longitudinal SPR peak blue-shifts around 10 nm per hour. After 8 hours, the etching rate starts slowing down, as the longitudinal SPR peak only shifts 38 nm in the next 16 hours. Additional time (up to 4 days) yields no further change in the longitudinal peak position (Figure S1), and the AuNR shape starts to become irregular rather than shorter (Figure S2). One explanation for this behavior is the dual role of cysteamine; the cysteamine can act as both an etchant and a stabilizing ligand. The thiol group of cysteamine can form a strong bond with the gold atoms at the surface of the AuNR, potentially preventing further etching. At low concentration of cysteamine (5 mM), the rate of etching seems higher than the rate of surface coordination, which allows for significant

This journal is © The Royal Society of Chemistry 20xx

Please do not adjust margins

Please do not adjust margins

shortening of the nanorods before cysteamine eventually forms a complete passivating layer on the nanorods ends.

We then varied some conditions to test their effect on the etching efficacy of cysteamine. Carrying out the reaction at lower temperatures (50 or 60°C) results in a slower rate of AuNR etching (Figure S1). Using higher temperature (80°C) also leads to overall lower etching efficiency (Figure S1), making 70°C the optimum temperature for AuNR etching using cysteamine. Doubling the concentration of cysteamine (from 5 mM to 10 mM) does not lead to significant difference in etching (Figure S1). Finally, increasing the pH from 5.5 (ultrapure water) to 8 (ultrapure water + $NaHCO_3$) results in much faster etching initially (Figure S1), but leads to aggregation of the AuNRs within 2 hours. One possible explanation is that the amine of the cysteamine hydrochloride salt gets deprotonated under basic conditions, leading to a loss of electrostatic repulsion between AuNRs as it forms a passivating layer on the surface of the rods.

Because the rod shape is preserved during etching, this can be useful as a method to prepare shorter AuNRs with high monodispersity. Indeed, the initial monodispersity is preserved during cysteamine etching, as the standard deviation remains nearly unchanged (10% before etching to 12% afterwards). Making highly uniform shorter aspect ratio AuNRs is often challenging due to the nature of the synthesis. Silver ions are needed for symmetry breaking in order to obtain rods, but a higher concentration will also lead to longer AuNRs;[43] a low concentration is needed to get short AuNRs, but too low will lead to more spherical particles. This leads to a very narrow range of silver ion concentration that can result in short AuNRs. Starting from longer AuNRs and using cysteamine etching allows highly controlled fine-tuning of AuNRs using mild conditions.

Heating[28, 37, 44, 45] to 100°C as well as photothermal reshaping[46, 47] have both been proposed as methods of AuNR shortening. In order to confirm that the etching was the result of cysteamine and not simply heating the sample, control tests were performed by heating AuNRs without adding cysteamine and by adding cysteamine to AuNRs at room temperature (Figure S3). It was found that heating AuNRs led to no change in the longitudinal SPR peak position even after 24 hours at 70°C. At room temperature, cysteamine still led to a shift in the longitudinal SPR peak position, though at a much slower rate.

In the previously reported etching of small gold nanoclusters by cysteamine,[34, 35] it is hypothesized that the etching is a result of the thiolate group and can be performed with other thiol molecules. As a control, we tested mercaptopropionic acid, a small water-soluble thiol molecule comparable to cysteamine in size, and saw no change in the SPR peak after 24 hours (Figure S3). Thus this seems to indicate that the etching properties of cysteamine are not simply due to the presence of the thiol group. Reported etching procedures work by way of redox reaction; an oxidant in solution (such as hydrogen peroxide,[20, 21, 23-26] iodide,[19, 20] or oxygen[40]) oxidizes Au^0 from the surface of the AuNRs to Au^+ ions, ultimately leading to a decrease in the nanoparticle size. It has also been proposed that the $O_2^{\cdot-}$ radical is responsible for the etching that occurs.[23, 48] Since cysteamine, commonly used as a reductant in biological applications,[49] has greater potential as a reducing agent than as an oxidizing agent, we propose that cysteamine does not etch the AuNR directly; rather, it acts as a catalyst, reacting with oxygen first and reducing it to form the H_2O_2 which in turn is then capable of oxidizing the Au^0 atoms through the mechanism described by Chandrasekar.[26, 48] We thus propose the two following half-cell reactions for the oxidation of Au^0 to Au^{III} initiated by cysteamine in the presence of oxygen:

$$2\ HSCH_2CH_2NH_3^+Cl^- + O_2 \rightarrow (SCH_2CH_2NH_2)_2 + H_2O_2 + 2Cl^- + 2H^+ \quad (1)$$

$$2Au^0 + 3H_2O_2 + 8Cl^- + 6H^+ \rightarrow 2[Au^{III}Cl_4]^- + 6H_2O \quad (2)$$

The production of H_2O_2 by cysteamine while heating at 60 °C was verified using an iodometric assay.[50] The generation of an absorption peak at 360 nm confirmed the presence of H_2O_2 in solution after heating cysteamine in water for 6 h (Figure S4). This validates reaction (1) of our proposed mechanism. While the reaction (2) has already been reported in previous studies on Au^0 oxidation using H_2O_2, the reaction schemes involved bromide ions instead of chloride ions for the complexation of the Au^{3+} ions formed.[26, 36] Indeed, the only source of anions in these studies was CTAB. In this present work, we postulate that the chloride ions from cysteamine hydrochloride are the ones contributing to the complexation of the gold ions, because we observe etching even in the absence of CTAB (in the case of silica-coated AuNRs, vide infra).

This overall mechanism can also explain the observation made by Wang *et al*;[33] when studying the cysteamine etching of gold nanospheres, they found that a lack of oxygen led to no etching in the presence of cysteamine.

Cysteamine etching of silica-coated AuNRs

We next looked at how the etching process was affected by the presence of a silica coating on the AuNRs. Silica shells were grown either at the ends, on the sides, or as a complete shell around the AuNRs. The controlled placement of silica shells at different locations on both AuNRs[51] and Au bibyramids[52] has been used previously for the anisotropic deposition of Pd. However, its effect on etching of AuNRs has not been studied before. For all three morphologies, tests were carried out at 60°C and using 5 mM cysteamine. The change in longitudinal SPR peak position over time as well as change in AuNR size after 24 hours for each of these is shown in Figure 3. It should be noted that while tests of the unsilicated AuNRs were performed in an aqueous 5 mM CTAB solution, tests involving silicated AuNRs were performed in ethanol with no CTAB present. This was done because of the better solubility of the silicated AuNRs in ethanol. However, control tests indicated no difference in rate or extent of etching when water or ethanol was used as solvent (Figure S3). Previous studies reporting etching methods have suggested that CTAB is necessary for etching to be observed when using H_2O_2 or $HAuCl_4$ as etchants;[26, 53] once oxidized and removed, the Au^+ ions form a stable complex with the CTAB, preventing it from reducing back to Au^0 and reassembling on the AuNR surface. Other studies have proposed that thiols (e.g., mercaptoethanol) complex with Au^+ during the etching

Please do not adjust margins

Please do not adjust margins

of spherical gold nanoparticles.[54] Thus it is likely that CTAB is not necessary in the present study because cysteamine is using its chloride counterion (since the ammonium chloride slat form of cysteamine is used here) to complex the Au^+ ions once they have been removed from the surface of the nanorod.

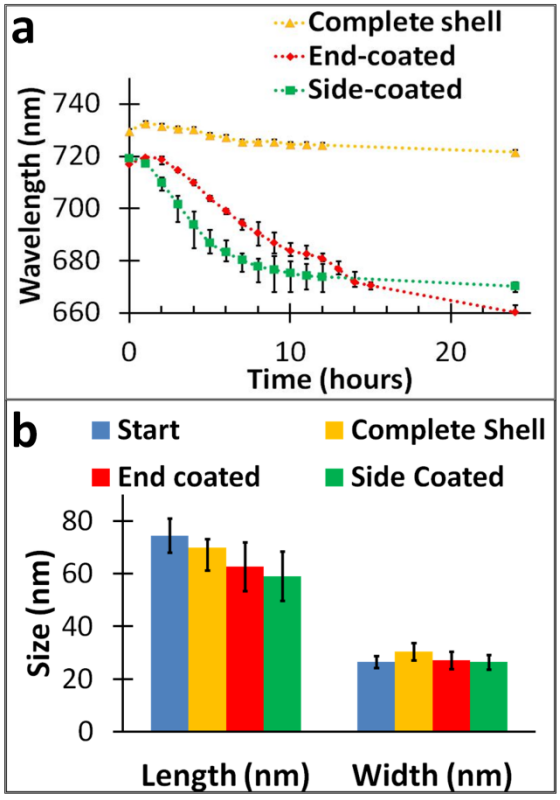

Figure 3. Comparison of etching effect on fully silica-coated AuNRs, silica end-coated AuNRs and silica side-coated AuNRs using 5 mM cysteamine at 60°C. Each etching experiment was done in triplicate. **(a)** Change in longitudinal surface plasmon peak position with time. Data points are the average of three trials. Error bars represent the minimum and maximum of the three trials. **(b)** Length and width measured from TEM images of starting AuNRs as well as after 24 hours of etching. Error bars show the standard deviation.

In the case of AuNRs surrounded by a complete shell of silica, little change was observed even 24 hours after cysteamine addition (Figure 3). The average of the three trials had a decrease in the longitudinal surface plasmon resonance (LSPR) peak position from 730 nm to 722 nm, corresponding to a 5 nm decrease in length (Table 1) indicating that the etching occurs at a drastically reduced rate when compared to the unsilicated AuNRs. Representative TEM images are shown in Figure 4(a). The complete silica shell around the AuNRs considerably restricts access to the surface gold atoms by cysteamine (and even the hydrogen peroxide responsible for the etching according to the proposed mechanism). However, it is still possible for cysteamine and H_2O_2 to slowly diffuse through the silica shell and induce some etching over time, given the mesoporous nature of the silica shells.[51, 55, 56]

The AuNRs with silica side-coating showed a dramatic change both in the longitudinal SPR peak position and in its size after 24 hours of etching, comparable to the unsilicated AuNRs (Figure 3). This is to be expected, given that the etching occurs preferentially at the end of the AuNRs and the ends of the AuNRs are exposed in this case. We see the same trend as in the unsilicated AuNRs where there is a rapid decline, after which the peak wavelength levels off and no further change is observed. However, in the case of the side-coated AuNRs, the inflection point appears sooner, both in terms of time and wavelength reached. Based on TEM images (shown in Figure 4(c,d)) it appears that as the etching occurs, the silica shell from the sides closes in around the ends leading to a complete silica shell around the etched AuNRs. Based on tests on AuNRs with a complete silica shell (*vide supra*), the completion of the silica shell is expected to lead to a dramatic decrease in the rate of any etching, consistent with our observations.

Table 1. Dimensions of AuNRs with different coatings after cysteamine etching.

	Length (nm)	Width (nm)	Tip Length (nm)
Start	74.9 +/- 7.2	26.5 +/- 2.8	6.0 +/- 1.5
CTAB (5 mM)	55.0 +/- 6.6	23.2 +/- 2.8	5.8 +/- 1.2
Complete shell (5 mM)	69.9 +/- 9.3	30.4 +/- 2.7	7.5 +/- 1.6
Side-coated (5 mM)	59.1 +/- 9.4	26.5 +/- 2.8	7.0 +/- 1.8
End-coated (5 mM)	62.7 +/- 9.3	27.2 +/- 3.3	9.8 +/- 2.3
Side-coated (53 mM)	59.4 +/- 10.7	25.4 +/- 2.6	11.2 +/- 2.2
End-coated (53 mM)	74.3 +/- 11.2	28.2 +/- 3.2	11.3 +/- 2.5
Side-coated (221 mM)	65.3 +/- 7.3	25.1 +/- 2.8	8.2 +/- 1.8
End-coated (221 mM)	84.6 +/- 5.6	27.3 +/- 1.3	8.3 +/- 1.9

In the case of the silica end-coated AuNRs, TEM analysis indicates that etching still occurs preferentially from the end of the rods, in spite of the presence of the silica caps at the ends of the rods while their sides are exposed. The length of the AuNRs decreases from 75 nm to 63 nm in the course of 24 hours while there is no significant change in the width of the rods during this time. This result can be understood in terms of the relative stabilities of the various crystal facets on the surfaces of the AuNRs. It has been proposed that CTAB influences AuNR surface reactivity not only by sterically blocking the surface, but also by decreasing the surface energy of high energy

This journal is © The Royal Society of Chemistry 20xx

Please do not adjust margins

Please do not adjust margins

facets.[14, 27, 30, 31, 57] In the case of the silica end-coated AuNRs, CTAB has been displaced by silica at the ends of the rods while remaining on the sides of the rods. Consequently, the lower stability of the facets located at the nanorod ends still allows for preferential etching at the nanorod ends, even though the ends appear to be more sterically hindered by the presence of the silica shell. In addition, the fact that silica is mesoporous and that its shell is thinning towards the rod sides might facilitate access of cysteamine from the sides to the ends.

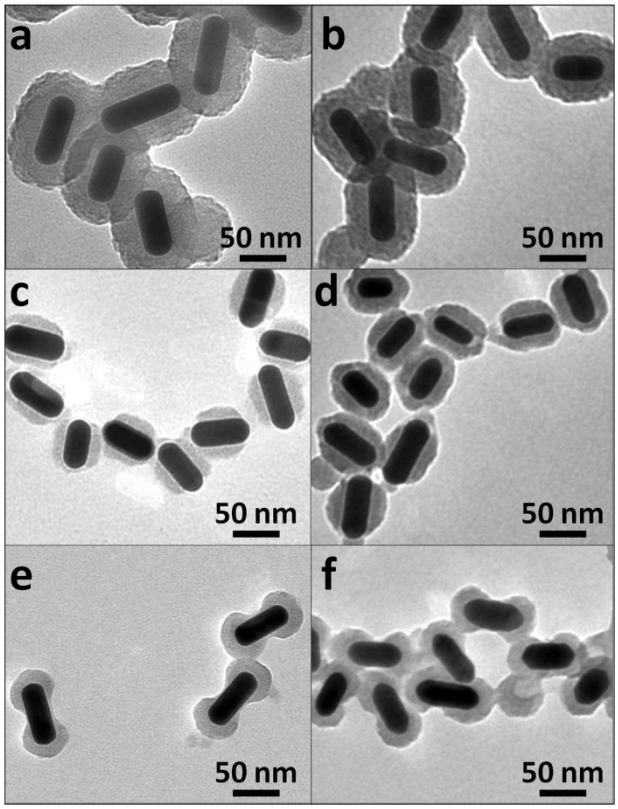

Figure 4. Etching of several types of silica-coated AuNRs using 5 mM cysteamine at 60°C for 24 hours. TEM images before **(a, c, e)** and after etching **(b, d, e)** of: AuNRs with complete silica shell **(a, b)**, silica side-coated AuNRs **(c, d),** and silica end-coated AuNRs **(e, f)**.

Nevertheless, we can notice, in Figure 3a, that the silica end-coated AuNRs take longer to show the effect of etching in comparison to the silica side-coated rods which show a plasmon peak shift almost immediately. This is consistent with access of cysteamine to the nanorod ends being slowed down by the presence of the SiO_2 end caps, whereas the ends of silica-side coated AuNRs are exposed and easily reached by cysteamine.

Perhaps more interestingly, in the case of the silica end-coated AuNRs, a change in the morphology of the tips is observed as etching occurs. Figure 4(e,f) shows a sample of end-coated AuNRs before and after etching with cysteamine. After etching, the nanorod tips become elongated and sharper. This is highlighted in Figure 5. A larger batch of AuNRs is also displayed in Figure S5, which shows that all AuNRs are sharpened to some extent, and that the degree of sharpening varies from rod to rod. In order to quantitatively compare the extent of sharpening between samples, we measure the tip length of the rods. We define tip length as the distance from the end of the rod to the end of the cylindrical part of the rod. Figure S6 shows a pictorial representation of this.

The average length of the tips increases from 6.0 nm to 9.8 nm (Table 1) while the rods as a whole are shorter. We propose that this is due in large part to the absence of CTAB during etching. It is understood that CTAB helps to increase the relative stability of higher energy [100] facets during nanorods formation, leading to the elongation of spherical particles into rods.[57] On the other hand, it is known that [111] facets are the most stable in colloidal gold in the absence of CTAB.[27, 29, 30, 57] Additionally, it has been previously observed that in the absence of CTAB, overgrowth of AuNRs by reduction of additional $HAuCl_4$ will lead to the disappearance of more reactive end facets and the growth of stable [111] facets so that arrow-head AuNRs, and eventually, octahedra form. [27,29]

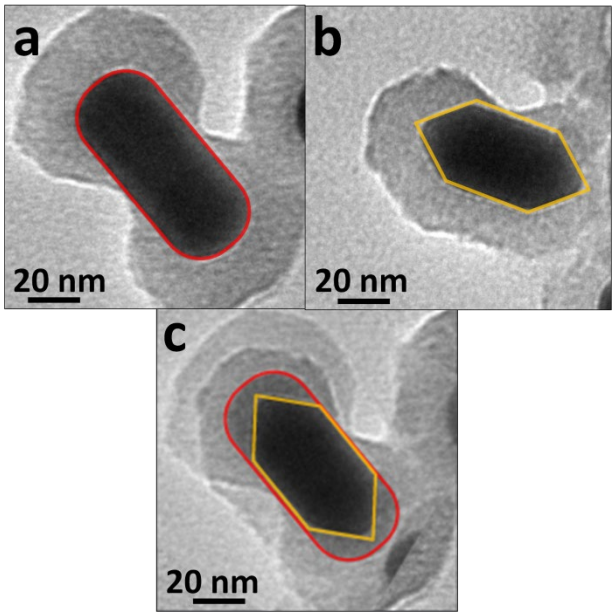

Figure 5. Magnified image of a single silica end-coated AuNR before **(a)** and after **(b)** etching with cysteamine (5 mM, 60°C, 24 hours). **(c)** Overlay of outlines of the two AuNRs from (a) and (b), highlighting the difference in tip shape before and after etching.

We propose that the reshaping of AuNR tips during etching with cysteamine follows the same principles; but rather than growing into [111] facets, as etching occurs, more reactive facets will be etched first, leaving four [111] facets which form the pointed tip of the AuNRs. We do not observe this reshaping in the case of the unsilicated AuNRs because CTAB decreases the difference in reactivity between the higher and lower energy facets at the ends of the AuNRs, which results in indiscriminate etching.

The absence of an observable change in the tip morphology after etching the silica side-coated AuNRs is more challenging to explain.

This journal is © The Royal Society of Chemistry 20xx

Please do not adjust margins

Please do not adjust margins

Indeed the measured length of the tips is not significantly changed (6 to 7 nm). A possible explanation could be the thiolated polyethylene glycol (HS-PEG-OMe) ligand used during the preparation of silica side-coated AuNRs. Prior to the SiO_2 side-coating, HS-PEG-OMe is added through ligand exchange of CTAB to block the ends of the AuNRs so that silica is only deposited on the sides. However it has been shown that ligand exchange of CTAB-stabilized AuNRs often is ineffective at completely removing CTAB,[58] especially in cases where large ligands such as PEG are used.[59] Thus the remaining CTAB still present at the ends most probably helps to increase the stability of the higher energy facets, leading to more homogenous etching.

In order to better understand the limits of etching of silica-coated AuNR using cysteamine, we assess the effect of using 10 times (53 mM) and 44 times (221 mM) higher cysteamine concentrations. Using a cysteamine concentration of 53 mM, the resulting silica side-coated AuNRs do display a more significant change in the tip morphology, becoming sharper: Figure 6 shows silica side-coated AuNRs etched with 53 mM cysteamine compared with the same AuNRs etched using 5 mM cysteamine. The tips of the AuNRs etched with 53 mM cysteamine increase in length from an average of 7 nm to 11 nm (Table 1). While no sharpening is observed at lower cysteamine concentrations due to the presence of residual CTAB, it is plausible that the sharpening at high concentration is due to the large excess of cysteamine, which is not only playing the role of etching agent but also the role of a strong stabilizing ligand with Au surface atoms. It is thus able to displace not only the HS-PEG-OMe from the AuNR surface but also any residual CTAB.

The use of 53 mM cysteamine for etching silica end-coated AuNRs also leads to a more pronounced sharpening than when using 5 mM cysteamine, with an increase in the AuNRs tip length from 9 nm to 11 nm (Table 1). However, we also notice that in this case the average length of the AuNRs stays essentially the same as the starting length (74 nm), whereas silica end-coated AuNRs etched with 5 mM cysteamine display an average length of 63 nm. In addition, the resulting etched AuNRs do not display a SiO_2 coating anymore. It seems that this higher concentration of cysteamine is able to displace the silica caps from the ends of the rods: this hypothesis is supported by a STEM picture showing a AuNR with one of the silica caps away from the rod's end (Figure S7). Further increasing the concentration of cysteamine to 220 nM also keeps the nanorod length unchanged, and leads to shorter tips (average of 8 nm) than using lower cysteamine concentrations. These results can be explained in terms of the dual-role nature of the cysteamine. We hypothesize that, at such high concentrations, the role of cysteamine as a ligand takes over its etching abilities, with the rate of passivation of the nanorods surface being much higher than the etching rate. The etching of gold by cysteamine at low concentrations provides justification for the use of a large excess of thiolated ligands to stabilize gold nanoparticles in solution. We observe the same general trend for silica side-coated AuNRs, where increasing the cysteamine concentration to 53 mM first leads to greater sharpening of the rods, but further cysteamine concentration increase (221 mM) leads to less sharpening and a decrease in etching.

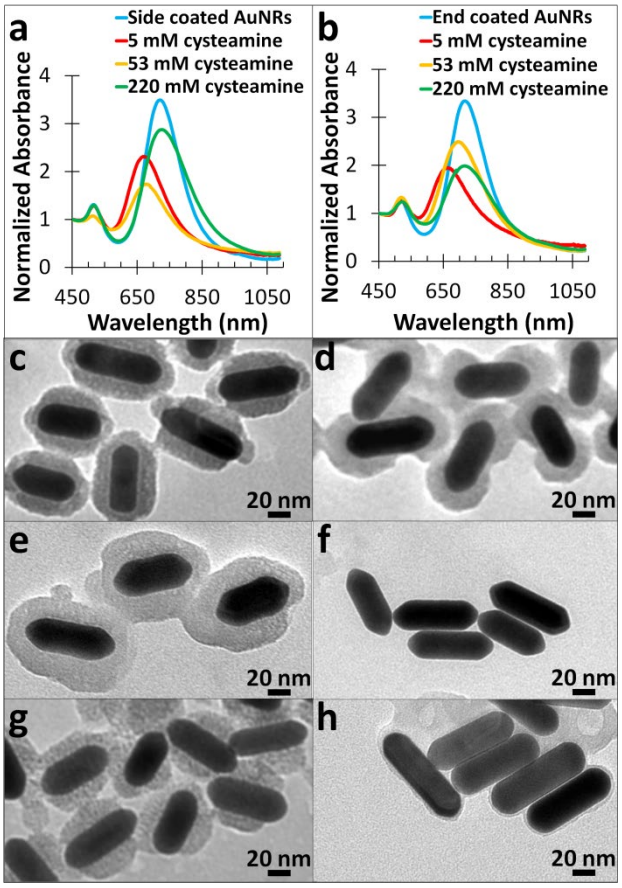

Figure 6. Cysteamine concentration-dependence of etching on silica-coated AuNRs. UV-vis spectra for **(a)** silica side-coated AuNRs and **(b)** silica end-coated AuNRs 24 hours after addition of different concentrations of cysteamine. TEM images show AuNRs etched with 5 mM cysteamine **(c, d),** 53 mM cysteamine **(e, f),** 220 mM cysteamine **(g, h).**

Single-particle scattering measurements

Finally, we performed measurements of the optical scattering spectra from single particles, and correlated the optical measurements with electron-microscope imaging of the same particles and simulations of the local surface-plasmon field enhancement. Figure 7 shows results for such analysis. The nanorod, a silica side-coated AuNR etched with 53 mM cysteamine, was imaged using STEM and its scattering spectra was measured afterwards. Simulations were performed for an AuNR geometry that matched the measured STEM image. In Figure 7, we can notice that the experimental measurement matches much better with the simulation of the sharpened AuNR than with the unsharpened AuNR of the same size, providing evidence of the change in morphology. The local field intensity enhancement factor (defined as $|E|^2/|E_0|^2$, where $|E_0|$ is the incident intensity) is enhanced from 780 in the unsharpened rod to 2,920 in the sharpened one. This means that cysteamine etching can be used not only to adjust the length of AuNRs post-synthesis, but it can also be used to enhance the local field at the tips of the nanorods. This can be useful for a variety of

 This journal is © The Royal Society of Chemistry 20xx

Please do not adjust margins

Please do not adjust margins

applications such as achieving greater fluorescence enhancement, coupling in nanoparticle assemblies, or SERS.

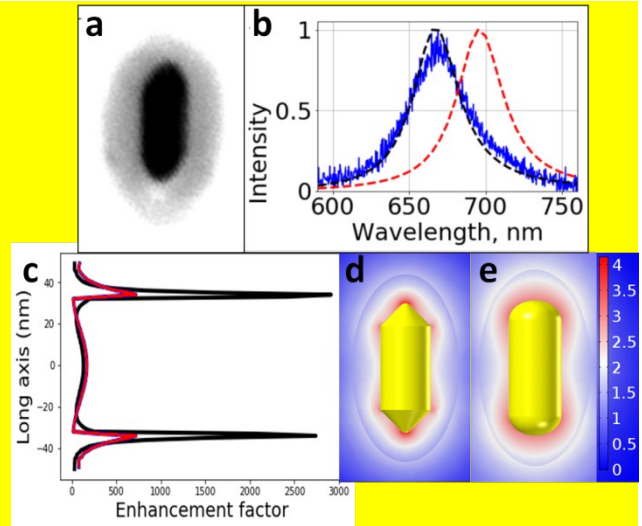

Figure 7. Single-particle study of AuNRs. **(a)** STEM image of a silica side-coated AuNR etched with 44 mM cysteamine for 24 hours, **(b)** Single-particle scattering measurement of the AuNR depicted in (a) (blue), as well as simulated scattering spectra for an AuNR matching the size and end-shape seen in (a) (black), and for an AuNR matching the size of the one seen in (a) but with typical as-synthesized end morphology (red). **(c)** Calculated enhancement along the long axis of the simulated AuNR for sharpened (black curve) and unsharpened (red curve) AuNR. **(d)** Simulated electric field for a single AuNR matching the dimensions and shape seen in (a) and corresponding to black curves in (b) and (c). **(e)** Simulated electric field for a single AuNR matching the dimensions seen in (a) but with typical unetched end-curvature, and corresponding to red curves in (b) and (c).

Conclusions

We have shown that cysteamine can be used at low concentration as an effective etchant for AuNRs. Cysteamine etches AuNRs preferentially from the ends in a controllable and reproducible manner, making it convenient for the post-synthesis fine-tuning of AuNR size and therefore optical properties. Unlike previously published methods of AuNR etching, our method can be performed in the absence of CTAB and does not rely on the presence of metal ions, strong acids, or strong oxidants. Furthermore, we study for the first time the etching of silica-coated AuNRs, and report that, under specific conditions, cysteamine can be used to sharpen the AuNR tips. This sharpening can be controlled by varying certain parameters, for example the concentration of cysteamine used and the location of the silica on the AuNRs, to obtain AuNRs with precisely tailored length and tip shapes. This is useful in the control of AuNR optical properties as well as for the enhancement of the local surface plasmon field at the ends of AuNRs for use in SERS and other applications. Finally, the remaining presence of cysteamine on the AuNRs after etching represents an additional benefit, as its terminal amino group provides an anchoring point for further coupling of AuNRs with other entities of interest.[60]

Conflicts of interest

There are no conflicts to declare.

Acknowledgements

This project was supported by the National Institute of Standards and Technology under Award Number 14D295 and by the National Science Foundation under Award Number CHE 1507462. The authors wish to thank Dr. Tagide deCarvalho for her help with TEM imaging at the UMBC Keith R. Porter Imaging Facility and Dr. Laszlo Takacs for his help with STEM imaging at the UMBC NanoImaging Facility (NIF).

References

1. Huang, X.; El-Sayed, I. H.; Qian, W.; El-Sayed, M. A., Cancer Cell Imaging and Photothermal Therapy in the Near-Infrared Region by Using Gold Nanorods. *Journal of the American Chemical Society* **2006,** *128* (6), 2115-2120.
2. Haine, A.; Niidome, T., Gold Nanorods as Nanodevices for Bioimaging, Photothermal Therapeutics, and Drug Delivery. *Chemical & Pharmaceutical Bulletin* **2017,** *65* (7), 625-628.
3. Parab, H. J.; Jung, C.; Lee, J.-H.; Park, H. G., A gold nanorod-based optical DNA biosensor for the diagnosis of pathogens. *Biosensors and Bioelectronics* **2010,** *26* (2), 667-673.
4. Niidome, T.; Yamagata, M.; Okamoto, Y.; Akiyama, Y.; Takahashi, H.; Kawano, T.; Katayama, Y.; Niidome, Y., PEG-modified gold nanorods with a stealth character for in vivo applications. *Journal of Controlled Release* **2006,** *114* (3), 343-347.
5. Zhou, J.; Cao, Z.; Panwar, N.; Hu, R.; Wang, X.; Qu, J.; Tjin, S.; Xu, G.; Yong, K., Functionalized gold nanorods for nanomedicine: Past, present and future. *Coordination Chemistry Reviews* **2017,** *352*, 15-66.
6. Hu, X.; Cheng, W.; Wang, T.; Wang, Y.; Wang, E.; Dong, S., Fabrication, Characterization, and Application in SERS of Self-Assembled Polyelectrolyte−Gold Nanorod Multilayered Films. *The Journal of Physical Chemistry B* **2005,** *109* (41), 19385-19389.
7. Zijlstra, P.; Chon, J. W. M.; Gu, M., Five-dimensional optical recording mediated by surface plasmons in gold nanorods. *Nature* **2009,** *459*, 410.
8. Hoggard, A.; Wang, L.; Ma, L.; Fang, Y.; You, G.; Olson, J.; Liu, Z.; Chang, W.; Ajayan, P.; Link, S., Using the Plasmon Linewidth To Calculate the Time and Efficiency of Electron Transfer between Gold Nanorods and Graphene. *Acs Nano* **2013,** *7* (12), 11209-11217.
9. Joplin, A.; Jebeli, S.; Sung, E.; Diemler, N.; Straney, P.; Yorulmaz, M.; Chang, W.; Millstone, J.; Link, S., Correlated Absorption and Scattering Spectroscopy of Individual Platinum-Decorated Gold Nanorods Reveals Strong Excitation Enhancement in the Nonplasmonic Metal. *Acs Nano* **2017,** *11* (12), 12346-12357.
10. Liu, Q.; Cui, Y.; Gardner, D.; Li, X.; He, S.; Smalyukh, I. I., Self-Alignment of Plasmonic Gold Nanorods in Reconfigurable Anisotropic Fluids for Tunable Bulk Metamaterial Applications. *Nano Letters* **2010,** *10* (4), 1347-1353.
11. Wang, P.; Liu, M.; Gao, G.; Zhang, S.; Shi, H.; Li, Z.; Zhang, L.; Fang, Y., From gold nanorods to nanodumbbells: a different way to tailor surface plasmon resonances by a chemical route. *Journal of Materials Chemistry* **2012,** *22* (45), 24006-24011.
12. Jiao, Z.; Xia, H.; Tao, X., Modulation of Localized Surface Plasmon Resonance of Nanostructured Gold Crystals by Tuning Their Tip Curvature with Assistance of Iodide and Silver(I) Ions. *The Journal of Physical Chemistry C* **2011,** *115* (16), 7887-7895.
13. Grzelczak, M.; Sánchez-Iglesias, A.; Rodríguez-González, B.; Alvarez-Puebla, R.; Pérez-Juste, J.; Liz-Marzán, L. M., Influence of Iodide Ions on the Growth of Gold Nanorods: Tuning Tip Curvature and Surface Plasmon Resonance. *Advanced Functional Materials* **2008,** *18* (23), 3780-3786.
14. Chen, H.; Shao, L.; Li, Q.; Wang, J., Gold nanorods and their plasmonic properties. *Chemical Society Reviews* **2013,** *42* (7), 2679-2724.
15. Jana, N. R.; Gearheart, L.; Murphy, C. J., Wet Chemical Synthesis of High Aspect Ratio Cylindrical Gold Nanorods. *The Journal of Physical Chemistry B* **2001,** *105* (19), 4065-4067.
16. Nikoobakht, B.; El-Sayed, M. A., Preparation and Growth Mechanism of Gold Nanorods (NRs) Using Seed-Mediated Growth Method. *Chemistry of Materials* **2003,** *15* (10), 1957-1962.
17. Ye, X.; Zheng, C.; Chen, J.; Gao, Y.; Murray, C. B., Using Binary Surfactant Mixtures To Simultaneously Improve the Dimensional Tunability and Monodispersity in the Seeded Growth of Gold Nanorods. *Nano Letters* **2013,** *13* (2), 765-771.
18. Burrows, N. D.; Harvey, S.; Idesis, F. A.; Murphy, C. J., Understanding the seed-mediated growth of gold nanorods through a fractional factorial design of experiments. *Langmuir* **2016,** *33* (8), 1891-1907.

Please do not adjust margins

Please do not adjust margins

19. Zhang, Z.; Chen, Z.; Wang, S.; Cheng, F.; Chen, L., Iodine-Mediated Etching of Gold Nanorods for Plasmonic ELISA Based on Colorimetric Detection of Alkaline Phosphatase. *ACS Applied Materials & Interfaces* **2015,** *7* (50), 27639-27645.
20. Zhang, Z.; Chen, Z.; Chen, L., Ultrasensitive Visual Sensing of Molybdate Based on Enzymatic-like Etching of Gold Nanorods. *Langmuir* **2015,** *31* (33), 9253-9259.
21. Ni, W.; Kou, X.; Yang, Z.; Wang, J., Tailoring Longitudinal Surface Plasmon Wavelengths, Scattering and Absorption Cross Sections of Gold Nanorods. *ACS Nano* **2008,** *2* (4), 677-686.
22. Sreeprasad, T. S.; Samal, A. K.; Pradeep, T., Body- or Tip-Controlled Reactivity of Gold Nanorods and Their Conversion to Particles through Other Anisotropic Structures. *Langmuir* **2007,** *23* (18), 9463-9471.
23. Zhang, Z.; Chen, Z.; Pan, D.; Chen, L., Fenton-like Reaction-Mediated Etching of Gold Nanorods for Visual Detection of Co2+. *Langmuir* **2015,** *31* (1), 643-650.
24. Liu, X.; Zhang, S.; Tan, P.; Zhou, J.; Huang, Y.; Nie, Z.; Yao, S., A plasmonic blood glucose monitor based on enzymatic etching of gold nanorods. *Chemical Communications* **2013,** *49* (18), 1856-1858.
25. Chen, Z.; Liu, R.; Wang, S.; Qu, C.; Chen, L.; Wang, Z., Colorimetric sensing of copper(ii) based on catalytic etching of gold nanorods. *RSC Advances* **2013,** *3* (32), 13318-13323.
26. Chandrasekar, G.; Mougin, K.; Haidara, H.; Vidal, L.; Gnecco, E., Shape and size transformation of gold nanorods (GNRs) via oxidation process: A reverse growth mechanism. *Applied Surface Science* **2011,** *257* (9), 4175-4179.
27. Carbó-Argibay, E.; Rodríguez-González, B.; Pacifico, J.; Pastoriza-Santos, I.; Pérez-Juste, J.; Liz-Marzán, L. M., Chemical Sharpening of Gold Nanorods: The Rod-to-Octahedron Transition. *Angewandte Chemie International Edition* **2007,** *46* (47), 8983-8987.
28. Gou, L.; Murphy, C. J., Fine-Tuning the Shape of Gold Nanorods. *Chemistry of Materials* **2005,** *17* (14), 3668-3672.
29. Xiang, Y.; Wu, X.; Liu, D.; Feng, L.; Zhang, K.; Chu, W.; Zhou, W.; Xie, S., Tuning the Morphology of Gold Nanocrystals by Switching the Growth of {110} Facets from Restriction to Preference. *The Journal of Physical Chemistry C* **2008,** *112* (9), 3203-3208.
30. Zhang, Q.; Han, L.; Jing, H.; Blom, D. A.; Lin, Y.; Xin, H. L.; Wang, H., Facet Control of Gold Nanorods. *ACS Nano* **2016,** *10* (2), 2960-2974.
31. Zhang, Q.; Zhou, Y.; Villarreal, E.; Lin, Y.; Zou, S.; Wang, H., Faceted Gold Nanorods: Nanocuboids, Convex Nanocuboids, and Concave Nanocuboids. *Nano Letters* **2015,** *15* (6), 4161-4169.
32. Liu, R.; Chen, Z.; Wang, S.; Qu, C.; Chen, L.; Wang, Z., Colorimetric sensing of copper(II) based on catalytic etching of gold nanoparticles. *Talanta* **2013,** *112*, 37-42.
33. Wang, H.; Goodrich, G. P.; Tam, F.; Oubre, C.; Nordlander, P.; Halas, N. J., Controlled Texturing Modifies the Surface Topography and Plasmonic Properties of Au Nanoshells. *The Journal of Physical Chemistry B* **2005,** *109* (22), 11083-11087.
34. Shu, T.; Su, L.; Wang, J.; Li, C.; Zhang, X., Chemical etching of bovine serum albumin-protected Au25 nanoclusters for label-free and separation-free detection of cysteamine. *Biosensors and Bioelectronics* **2015,** *66* (Supplement C), 155-161.
35. Shu, T.; Su, L.; Wang, J.; Lu, X.; Liang, F.; Li, C.; Zhang, X., Value of the Debris of Reduction Sculpture: Thiol Etching of Au Nanoclusters for Preparing Water-Soluble and Aggregation-Induced Emission-Active Au(I) Complexes as Phosphorescent Copper Ion Sensor. *Analytical Chemistry* **2016,** *88* (11), 6071-6077.
36. Wen, T.; Zhang, H.; Tang, X.; Chu, W.; Liu, W.; Ji, Y.; Hu, Z.; Hou, S.; Hu, X.; Wu, X., Copper Ion Assisted Reshaping and Etching of Gold Nanorods: Mechanism Studies and Applications. *The Journal of Physical Chemistry C* **2013,** *117* (48), 25769-25777.
37. Liu, Y.; Mills, E. N.; Composto, R. J., Tuning optical properties of gold nanorods in polymer films through thermal reshaping. *Journal of Materials Chemistry* **2009,** *19* (18), 2704-2709.
38. Zhang, Z.; Chen, Z.; Qu, C.; Chen, L., Highly Sensitive Visual Detection of Copper Ions Based on the Shape-Dependent LSPR Spectroscopy of Gold Nanorods. *Langmuir* **2014,** *30* (12), 3625-3630.
39. Chen, Z.; Zhang, Z.; Qu, C.; Pan, D.; Chen, L., Highly sensitive label-free colorimetric sensing of nitrite based on etching of gold nanorods. *Analyst* **2012,** *137* (22), 5197-5200.
40. Tsung, C.-K.; Kou, X.; Shi, Q.; Zhang, J.; Yeung, M. H.; Wang, J.; Stucky, G. D., Selective Shortening of Single-Crystalline Gold Nanorods by Mild Oxidation. *Journal of the American Chemical Society* **2006,** *128* (16), 5352-5353.
41. Zou, R.; Guo, X.; Yang, J.; Li, D.; Peng, F.; Zhang, L.; Wang, H.; Yu, H., Selective etching of gold nanorods by ferric chloride at room temperature. *CrystEngComm* **2009,** *11* (12), 2797-2803.
42. Li, F.-M.; Liu, J.-M.; Wang, X.-X.; Lin, L.-P.; Cai, W.-L.; Lin, X.; Zeng, Y.-N.; Li, Z.-M.; Lin, S.-Q., Non-aggregation based label free colorimetric sensor for the detection of Cr (VI) based on selective etching of gold nanorods. *Sensors and Actuators B: Chemical* **2011,** *155* (2), 817-822.
43. Si, S.; Leduc, C.; Delville, M.-H.; Lounis, B., *Short Gold Nanorod Growth Revisited: The Critical Role of the Bromide Counterion*. 2012; Vol. 13, p 193-202.
44. Khee Chaw Ng and Wenlong, C., Fine-tuning longitudinal plasmon resonances of nanorods by thermal reshaping in aqueous media. *Nanotechnology* **2012,** *23* (10), 105602.
45. Mohamed, M. B.; Ismail, K. Z.; Link, S.; El-Sayed, M. A., Thermal Reshaping of Gold Nanorods in Micelles. *The Journal of Physical Chemistry B* **1998,** *102* (47), 9370-9374.
46. Hironobu Takahashi and Takuro Niidome and Ayuko Nariai and Yasuro Niidome and Sunao, Y., Photothermal reshaping of gold nanorods prevents further cell death. *Nanotechnology* **2006,** *17* (17), 4431.
47. Horiguchi, Y.; Honda, K.; Kato, Y.; Nakashima, N.; Niidome, Y., Photothermal Reshaping of Gold Nanorods Depends on the Passivating Layers of the Nanorod Surfaces. *Langmuir* **2008,** *24* (20), 12026-12031.
48. Dreier Timothy, A.; Ackerson Christopher, J., Radicals Are Required for Thiol Etching of Gold Particles. *Angewandte Chemie International Edition* **2015,** *54* (32), 9249-9252.
49. Thoene, J. G.; Oshima, R. G.; Crawhall, J. C.; Olson, D. L.; Schneider, J. A., Cystinosis. Intracellular cystine depletion by aminothiols in vitro and in vivo. *The Journal of Clinical Investigation* **1976,** *58* (1), 180-189.
50. DeLong, J. M.; Prange, R. K.; Hodges, D. M.; Forney, C. F.; Bishop, M. C.; Quilliam, M., Using a modified ferrous oxidation-xylenol orange (FOX) assay for detection of lipid hydroperoxides in plant tissue. *J Agric Food Chem* **2002,** *50* (2), 248-54.
51. Wang, F.; Cheng, S.; Bao, Z.; Wang, J., Anisotropic Overgrowth of Metal Heterostructures Induced by a Site-Selective Silica Coating. *Angewandte Chemie International Edition* **2013,** *52* (39), 10344-10348.
52. Zhu, X.; Jia, H.; Zhu, X.-M.; Cheng, S.; Zhuo, X.; Qin, F.; Yang, Z.; Wang, J., Selective Pd Deposition on Au Nanobipyramids and Pd Site-Dependent Plasmonic Photocatalytic Activity. *Advanced Functional Materials* **2017,** *27* (22), 1700016.
53. Rodríguez-Fernández, J.; Pérez-Juste, J.; Mulvaney, P.; Liz-Marzán, L. M., Spatially-Directed Oxidation of Gold Nanoparticles by Au(III)−CTAB Complexes. *The Journal of Physical Chemistry B* **2005,** *109* (30), 14257-14261.
54. Chen, Y.-Y.; Chang, H.-T.; Shiang, Y.-C.; Hung, Y.-L.; Chiang, C.-K.; Huang, C.-C., Colorimetric Assay for Lead Ions Based on the Leaching of Gold Nanoparticles. *Analytical Chemistry* **2009,** *81* (22), 9433-9439.
55. Luo, T.; Huang, P.; Gao, G.; Shen, G.; Fu, S.; Cui, D.; Zhou, C.; Ren, Q., Mesoporous silica-coated gold nanorods with embedded indocyanine green for dual mode X-ray CT and NIR fluorescence imaging. *Optics Express* **2011,** *19* (18), 17030-17039.
56. Hinman, J. G.; Eller, J. R.; Lin, W.; Li, J.; Li, J.; Murphy, C. J., Oxidation State of Capping Agent Affects Spatial Reactivity on Gold Nanorods. *Journal of the American Chemical Society* **2017,** *139* (29), 9851-9854.
57. Katz-Boon, H.; Walsh, M.; Dwyer, C.; Mulvaney, P.; Funston, A. M.; Etheridge, J., Stability of Crystal Facets in Gold Nanorods. *Nano Letters* **2015,** *15* (3), 1635-1641.
58. Mehtala, J. G.; Zemlyanov, D. Y.; Max, J. P.; Kadasala, N.; Zhao, S.; Wei, A., Citrate-Stabilized Gold Nanorods. *Langmuir* **2014,** *30* (46), 13727-13730.
59. Nguyen, T. M.; Gigault, J.; Hackley, V. A., PEGylated gold nanorod separation based on aspect ratio: characterization by asymmetric-flow field flow fractionation with UV-Vis detection. *Analytical and Bioanalytical Chemistry* **2014,** *406* (6), 1651-1659.
60. Hofmann, A.; Schmiel, P.; Stein, B.; Graf, C., Controlled Formation of Gold Nanoparticle Dimers Using Multivalent Thiol Ligands. *Langmuir* **2011,** *27* (24), 15165-15175.

 This journal is © The Royal Society of Chemistry 20xx

Please do not adjust margins